Molecular Structure and Properties of Ethylene-*co*-Styrene Polymers Obtained from [Norbornane-7,7-bis(1-indenyl)]titanium Dichloride Catalyst System

M. T. Expósito, J. F. Vega, J. Martínez-Salazar

Departamento de Física Macromolecular, Instituto de Estructura de la Materia, CSIC, Serrano 113 bis, 28006 Madrid, Spain

Received 16 March 2007; accepted 18 May 2007
DOI 10.1002/app.26797
Published online 12 July 2007 in Wiley InterScience (www.interscience.wiley.com).

ABSTRACT: Ethylene-*co*-styrene polymers have been synthesized using the new catalyst system [norbornane-7,7-bis(1-indenyl)]titanium dichloride, and characterized by SEC, ^{13}C-NMR, DSC, and dynamic-mechanical analysis. The copolymers have higher average molecular weights compared with those produced in our group with other single-site catalysts systems in the same conditions. More specifically, the homopolymers are ultra high molecular weight polyethylenes (molecular weight higher than 10^6 g mol^{-1}) and with a narrow molecular weight distribution. All samples have shown an unprecedented homogeneous chemical composition with a random incorporation of the comonomer during the polymerization. The expected relationship between thermal properties and the amount of comomoner related to the exclusion of the phenyl units from the crystalline structure has been found, but the correlation is slightly different from those found in other copolymers. This is likely due to the different molecular features of the copolymers. In addition, intense and narrow mechanical relaxations have been found in the samples tested, pointing towards an extremely homogeneous microstructure. The materials obtained show a conspicuous strain hardening during tensile deformation at high strains, not only related to the constrain imposed by the bulky phenyl group in the amorphous region, but additionally to the extremely high number of entanglements in this region as a consequence of the high molecular mass of the samples. © 2007 Wiley Periodicals, Inc. J Appl Polym Sci 106: 1421–1430, 2007

Key words: copolymerization; metallocene catalysts; mechanical properties; thermal properties

INTRODUCTION

The design and the modification of catalysts structure to enhance their abilities during polymerization are challenging in polymer science. This is specially interesting in the case of α-olefin copolymerization as a way to afford potential new materials with modified properties, better process ability, and compatibility with existing polymers.[1,2] The random copolymerization of ethylene with styrene has become possible with the use of single site catalysts (SSC). In this context, it was found 15 years ago constrained geometry catalysts (CGC) to be very active for the copolymerization of ethylene with a variety of comonomers, including styrene.[3–7] This fact is crucial since modifying the comonomer content, a wide range of material properties can be obtained.[8–14] In a recent study, we have demonstrated that the inclusion of the norbornane bicycle in the structure of an *ansa*-metallocene catalysts hinders the movement of the indenyl ligands. As a result, a highly stereorigid catalyst is obtained in which the geometry of the active center remains fixed all along the catalytic process. Details about the preparation and characteristics of this new catalyst can be found elsewhere.[15] The activity of this catalyst, [norbornane-7,7-bis(1-Ind)]$TiCl_2$(NIT), in ethylene/styrene copolymerization is one order of magnitude higher than with the commercial CGC catalyst, [(η^5-C_5Me_4)$SiMe_2$(N*tert*-Bu)]$TiCl_2$. The NIT catalyst is also much more active than other *ansa*-titanocenes and *ansa*-zirconocenes in the same polymerization conditions.[16] In addition, this new catalyst yields completely linear chains (without long chain branching), in contrast to the CGC catalyst, which seems to produce long chain branched (LCB) species under certain conditions.[17,18]

The present study concerns to the relationship between molecular architecture and thermal and mechanical properties of the ethylene-*co*-styrene polymers obtained with this new catalyst system. We also show the results obtained for a family of copolymers obtained in the same polymerization conditions using the half-sandwich CGC system.

Correspondence to: J. F. Vega (imtv477@iem.cfmac.csic.es).
Contract grant sponsor: CICYT; contract grant number: MAT2006-0400.

EXPERIMENTAL

Materials, synthesis, and preparation of the samples

We have carried out ethylene/styrene copolymerization with both NIT and CGC catalysts activated by methylaluminoxane (MAO) purchased from Witco (Germany, 10 wt % MAO in toluene) at several monomer-feeding ratios. The copolymerizations have been carried out in HPLC grade toluene (from Scharlau Chimie, France). Ethylene and nitrogen (purchased from Air Liquid, France) as well as toluene were further purified by passing through a series of columns containing molecular sieves and Al_2O_3, to remove residual traces of moisture and oxygen. All materials were handled and stored under dry nitrogen atmosphere. Polymerizations were performed in toluene and the required MAO co-catalyst under nitrogen atmosphere, in a 1 L glass autoclave (Büchi). The conditions used for all the experiments were [cat] = 20 μmol/L, Al:Ti = 2000, ethylene pressure = 3 bar, polymerization temperature = 35°C. Detailed polymerization procedures can be found elsewhere.[15–18]

The copolymers were stabilized using a mixture 1.0 wt % of Irganox 1010 and Irgafos 168 by mixing the copolymer and the antioxidants during compression molding. The copolymer was compression molded into a 1-mm thick plate. The polymer plates were sandwiched between metallic sheets, heated at 150°C, held for 3 min under a nominal pressure of 100 kg/cm^2, and cooled in the press from 150 to 30°C at a rate of 15°C/min. The same heating/cooling program was used to achieve a similar thermal history for all the compression-molded samples.

Characterization of the samples

Molecular features and microstructure

Average molecular weights M_w and M_n and molecular weight distributions were determined by size exclusion chromatography (SEC) in a 150 CV Waters GPC coupled with refractive index RI and viscosity detectors. The solvent used for the analysis was 1,2,4-trichlorobenzene (TCB), the flow rate was 1.0 mL/min and the temperature was 145°C. The SEC-viscosity system was calibrated using polystyrene standards. M_w and polydispersity index of the samples are listed in Tables I and II.

TABLE I
Molecular Properties of the Ethylene-*co*-Styrene Samples Obtained from the NIT Catalyst

Sample	Styrene content (% mol)	M_w (kg mol^{-1})	M_w/M_n
NIT000	0.0	2300	2.5
NIT010	1.0	610	2.9
NIT014	1.4	560	2.3
NIT019	1.9	660	2.6
NIT021	2.1	620	2.5
NIT024	2.4	395	2.0
NIT026	2.6	560	2.4
NIT029	2.9	340	2.0
NIT035	3.5	449	2.1
NIT041	4.1	325	1.9

TABLE II
Molecular Properties of the Ethylene-*co*-Styrene Samples Obtained from the CGC Catalyst

Sample	Styrene content (% mol)	M_w (kg mol^{-1})	M_w/M_n
CGC000	0.0	273	2.6
CGC004	0.4	212	2.2
CGC009	0.9	173	2.1
CGC020	2.0	138	3.2
CGC023	2.3	170	2.2
CGC031	3.1	91	2.0
CGC047	4.7	159	2.9
CGC053	5.3	164	2.3
CGC103	10.3	n.d.	n.d.
CGC115	11.5	120	2.0

All the samples were analyzed by ^{13}C-NMR. Spectra were recorded at 100°C on a Bruker DRX 500 spectrometer operating at 500 MHz. The samples were dissolved in hot TCB and d^6-benzene. Carbon signals and styrene contents (Tables I and II) were assigned according to the literature.[12]

Chemical composition distributions of the copolymers were determined with a CRYSTAF/TREF instrument model 200+ (Polymer ChAR, Spain) equipped with five separate crystallization vessels for simultaneously analyze five different samples. Samples of 21 mg were dissolved in 30 mL of TCB at a temperature of 160°C for a total time of 135 min. Then the solutions were allowed to reach the thermal equilibrium at 95°C for another 45 min. Afterwards, the solutions were cooled at cooling rate of 0.2°C/min to 35°C. The different solutions were sampled 30 times at temperature intervals between 95 and 35°C, and the concentration of the remaining copolymer in the solutions was measured with a dual-wavelength infrared detector.

Thermal properties

A Perkin–Elmer DSC7 was used for the thermal analysis with indium as a calibration standard. For measurements, 7–10 mg round samples were punched out of the compression-molded polymer plates. The diameter of the samples (c.a. 4 mm) was adjusted to that of flat-based DSC pans, to achieve a constant geometry and good contact between the sample and pan. Melting exotherms were recorded

by heating the samples from 25 to 160°C at a heating rate of 10°C/min. Melting temperatures were obtained and crystallinity values were calculated from the heat of fusion using the area of the melting peak; a value of 288.4 J/g was used as the reference melting enthalpy for 100% crystalline polyethylene.[19]

Dynamic-mechanical analysis

For the dynamic-mechanical analysis, a Perkin-Elmer Dynamic Mechanical Analyzer DMA7 in the flexural mode coupled with dual cantilever geometry was used. Temperature calibrations were performed using the melting onset of water and indium. The storage and loss moduli, E' and E'', and the loss tangent, tan δ, at a frequency of 1 Hz were obtained in the temperature range from –60 to 120°C at a heating rate of 2°C min^{-1}. The applied dynamic strain amplitude was below 0.2%.

Also flexural dynamic stress-strain behavior of the samples was obtained by dynamic mechanical spectroscopy analysis in a Perkin–Elmer Dynamic Mechanical Analyzer DMA7 with double cantilever geometry at 20°C. Complex flexural modulus, $|E^*|$, and loss angle δ, at a frequency of 1 Hz were obtained in a range of flexural strain from 0.01 to 1%. For this investigation, rectangular shaped samples of about 15 mm × 5 mm × 1 mm were cut from the compression-molded sheets.

Mechanical properties

The stress–strain behavior in uniaxial tension at room temperature was also studied with a MTS universal testing machine with specimens cut from the plaques of about 1-mm thickness. The grip separation was 12 mm. Specimens were stretched at 2 strain rates (1 and 10 mm/min) at room temperature. Engineering strain was calculated from the crosshead displacement. Engineering stress was defined conventionally as the force per initial unit cross-sectional area.

RESULTS AND DISCUSSION

Molecular and microstructural features and chemical composition

Tables I and II summarize the molecular features of the copolymers studied. The molar mass distribution of all polymers investigated shows a low polydispersity index of $M_w/M_n \sim 2$–3, as it is characteristic of SSC. The products differ in weight mass average M_w, which in general slightly decreases as the incorporation of styrene in the copolymer increases, irrespective of the catalyst system used in the polymerization. The main difference between both set of polymer lies on the average molecular weight values. The copolymers obtained with NIT catalyst show much higher molecular weight than those obtained with CGC. The result obtained for the homopolymer (NIT000) is especially interesting. In this case, a very high molecular weight ($>10^6$ g mol^{-1}) is obtained. This is an ultra high molecular weight polyethylene (UHMWPE), which is suitable for very interesting applications, as this material has a unique combination of properties for the strongest wear and environmental circumstances and for its use as a wear face in orthopedic implants in joint replacements.

The ^{13}C-NMR spectra of the copolymers show the characteristic peaks with a chemical shift of 27.87, 29.98, 37.19, and 46.42 ppm, associated respectively to $S_{\beta\delta}$, $S_{\gamma\delta}$ ($S_{\delta\delta}$, $S_{\gamma\gamma}$), $S_{\alpha\delta}$, and $T_{\delta\delta}$ carbons of ethylene–ethylene sequences with isolated styrene units. These characteristic signals are observed in Figure 1(a) for the copolymers obtained using the NIT catalyst, and correspond to pure random distributions of styrene units. However, in those copolymers obtained with the CGC catalyst whose styrene con-

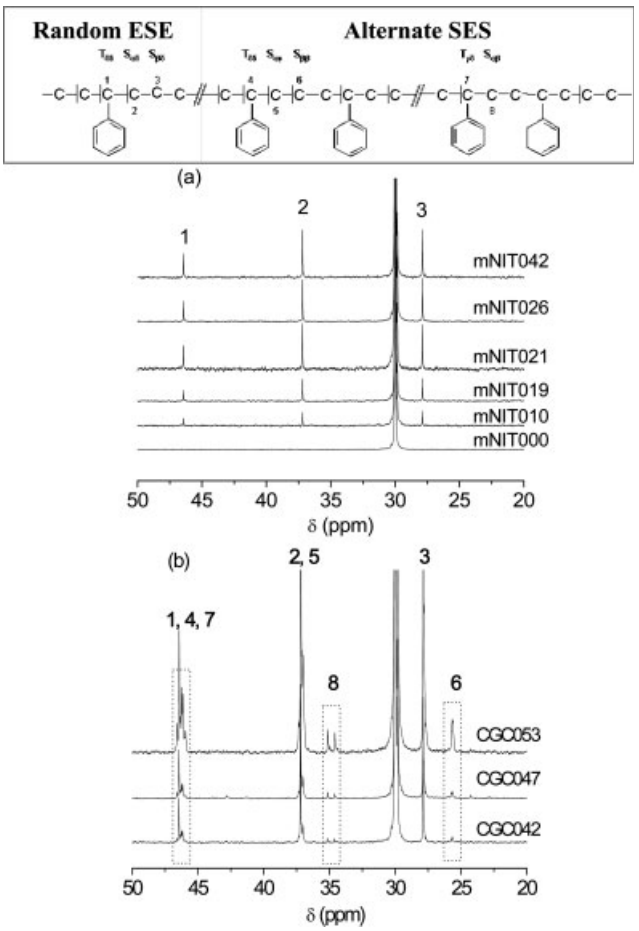

Figure 1 ^{13}C-NMR spectra of ethylene-*co*-styrene copolymers obtained from (a) NIT catalyst and (b) CGC catalyst.

tent is above 3.0 mol %, other resonances appear at 25.66, 36.99, and 46.15 ppm attributed to $S_{\beta\beta}$, $S_{\alpha\gamma}$, and $T_{\delta\delta}$ carbons of ethylene–styrene alternating sequences, and signals at 34.56 and 46.42 ppm corresponding to $S_{\alpha\beta}$ and $T_{\gamma\delta}$ carbons [Fig. 1(b)]. These latter additional signals observed in the CGC copolymers can be assigned to two coupling types of styrene units: tail to tail or head to head bridged by an ethylene unit, already reported in the literature.[8,9] These results have been confirmed by computational studies carried out in our group.[20] Thus, on the basis of the energy profiles, theoretical calculations showed that the secondary styrene insertion into Ti-1,2S species, giving rise to the tail to tail enchainment, is a process with a little probability from a kinetic point of view but is likely thermodynamically. Therefore, ethylene insertion into Ti-2,1S followed by a primary styrene insertion to give head to head styrene units bridged by an ethylene unit is also a likely process from a thermodynamically point of view with an energy barrier very similar to the latter mechanism. So, it is not possible to establish clearly the assignment of $S_{\alpha\beta}$ and $T_{\gamma\delta}$ carbons since these resonances could be due to both insertion mechanisms. All these facts indicate styrene is distributed in such a way the copolymer architecture is ''pseudo-random'' in the case of CGC copolymers.

The chemical homogeneity of the copolymers obtained by means of NIT catalyst has been confirmed by CRYSTAF analysis. The CRYSTAF profiles corresponding to some of the copolymers listed in Tables I and II are shown in Figure 2 for those obtained from the NIT catalyst, and in Figure 3 for those produced by the CGC catalyst. The narrow and symmetrical CRYSTAF profiles illustrated in Figure 2 clearly indicate that no drift takes place

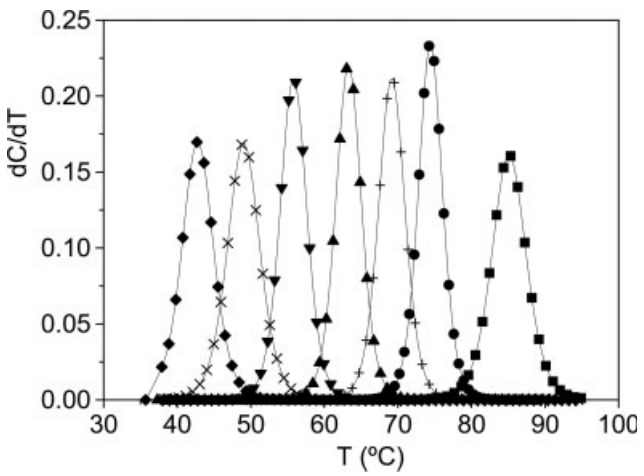

Figure 2 CRYSTAF profiles of some of the copolymers obtained from NIT catalyst studied: (■) NIT000, (●) NIT010; (+) NIT017 (▲) NIT025, (▼) NIT029, (×) NIT035, and (◆) NIT041.

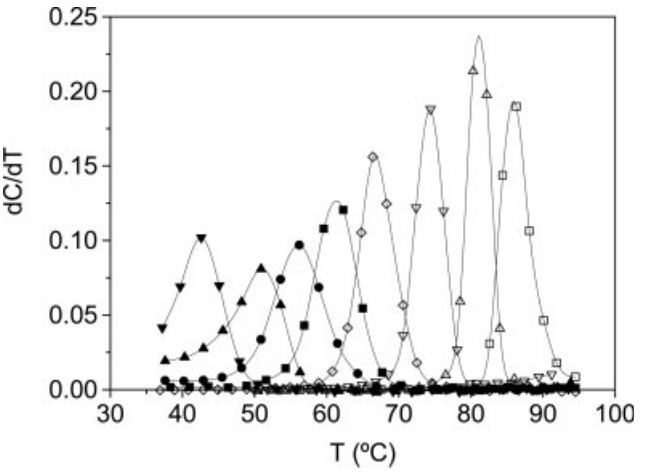

Figure 3 CRYSTAF profiles of selected ethylene-*co*-styrene samples studied: (□) CGC000; (△) CGC004, (▽) CGC009; (◇) CGC020; (■) CGC023; (●) CGC031; (▲) CGC042; (▼) CGC053.

during the polymerization reactions irrespective of styrene composition when the new NIT catalyst system is used. This feature points towards an extraordinary homogeneity in the chemical composition of the materials obtained with this catalyst. In addition, it is worthwhile to note that the copolymers obtained with this catalyst are very homogeneous from both molecular (polydispersity index close to 2) and micro structural (only random ethylene and styrene units by ^{13}C-NMR) points of view. The chemical composition of these copolymers seem to be much more homogeneous that those of the copolymers obtained by means from CGC catalyst in the same polymerization conditions and range of styrene content. The composition distribution of each sample can be described by means of the number and weight averages crystallization temperatures:

$$T_n = \frac{\sum_i C_i}{\sum_i \frac{C_i}{T_i}}; \quad T_w = \frac{\sum_i C_i T_i}{\sum_i C_i} \tag{1}$$

where C_i is the concentration of the polymer in solution at the temperature T_i. A measure of the breadth of the distribution can be measured by means of the standard deviation σ, defined as:

$$\sigma = \sqrt{\frac{\sum_i C_i (T_i^2 - T_w^2)}{\sum_i C_i}} \tag{2}$$

The standard deviation of the distribution in the copolymers obtained from NIT catalyst remains constant ($\sigma \sim 2$) in the whole range of comonomer content [Figs. 2 and 4(a)]. On the contrary, for CGC

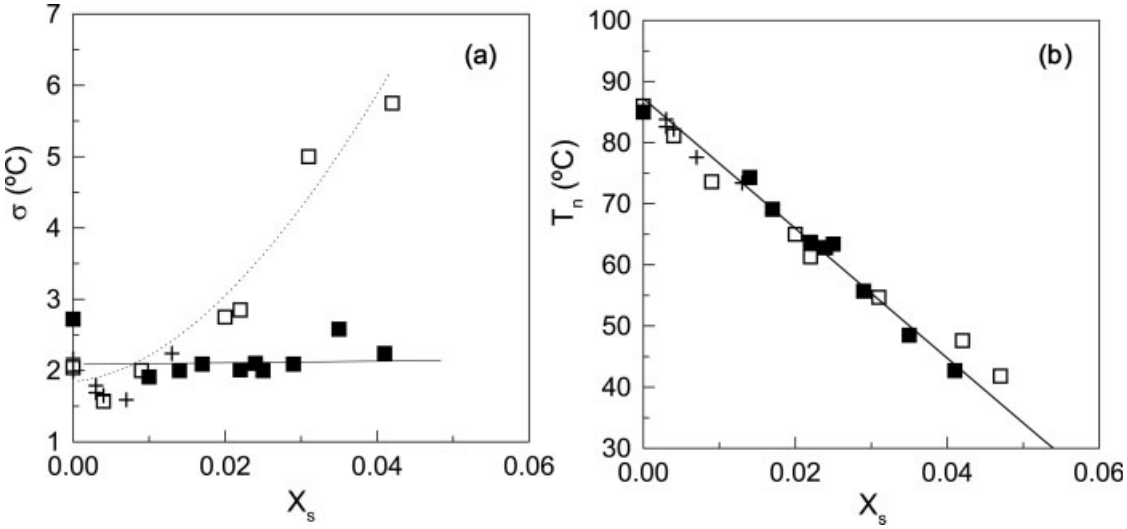

Figure 4 (a) Breath of the distributions and (b) number–average crystallization temperature obtained from CRYSTAF profiles for ethylene-*co*-styrene copolymers: (■) NIT copolymers; (□) CGC copolymers; (+) other copolymers obtained from metallocene catalysts.[15–18] Lines in (a) are drawn to guide the eye. The line in (b) has been determined by linear regression for NIT copolymers.

samples σ steeply increases with increasing comonomer incorporation, as it can be observed in Figures 3 and 4(a). This latter trend has been also observed in ethylene-*co*-1-hexene copolymers obtained by means of other SSC catalyst systems.[21–26] The increasing breadth of CRYSTAF profiles with increasing comonomer amount in the copolymer has been attributed to the broadening of the ethylene sequence lengths distribution between comonomer units. As the comonomer content increases in CGC copolymers, the chemical compositions distribution broadens, but norbornane-derived copolymers distributions remain very narrow. Then, the ethylene-*co*-styrene copolymers synthesized from NIT catalyst are useful as calibration standards for CRYSTAF as they all have narrow, monomodal composition distributions and cover a broad range of styrene incorporation. The linear relationship between the number average crystallization temperature, T_n, and the molar composition obtained from ^{13}C-NMR for the samples analyzed is illustrated in Figure 4(b). The figure includes some results obtained in our laboratory for ethylene-*co*-styrene copolymers.[16] Similar CRYSTAF calibration curves have been generated for α-olefin copolymers by other researchers. Monrabal et al. used a series of ethylene-*co*-1-octene copolymers[21] and Sarzotti et al. did the same for a family of ethylene-*co*-1-hexene copolymers,[22,26] both sets of materials synthesized with SSC. Although the calibration curves for CRYSTAF are likely instrument dependent it is interesting to note that the slope of the calibration curve found for ethylene-*co*-styrene (10.40) is very close to those obtained for ethylene-*co*-1-hexene (10.80 by Sarzotti et al.).[22]

Thermal properties

There is still a lack of systematic studies focusing on the melting behavior of copolymers of different styrene contents obtained using SSC catalysts. Arai et al.[13] and Venditto et al.,[14] and more recently also our group[16] examined ethylene-*co*-styrene copolymers prepared using different metallocene catalysts. Veneditto et al., reported two melting points at 85 and 125°C for a copolymer containing 13 mol % styrene, while Arai at al. obtained a homogeneous copolymer with only one melting point in the thermogram at 112°C for a copolymer with a styrene content of 9 mol %. We have also found non-homogeneity in both the melting and crystallization thermograms for copolymers obtained using SSC, indicating that the copolymers are a mixture of ethylene-*co*-styrene copolymers and polyethylene homopolymer or two ethylene-*co*-styrene copolymers with different styrene content.

The second melting thermograms of the some of copolymers produced using both catalysts are observed in Figure 5. It can be seen that the shape of the melting thermograms are influenced by the amount of styrene comonomer and catalyst type. This figure shows homogeneity in the melting peaks for NIT copolymers indicating homogeneous microstructure, even for the highest styrene contents. On the contrary, the copolymers obtained using the CGC catalyst show broader melting peaks, especially for the highest styrene content, for which a clear shoulder appears at low temperatures, indicating a more complex microstructure in agreement with ^{13}C-NMR results and CRYSTAF analysis.

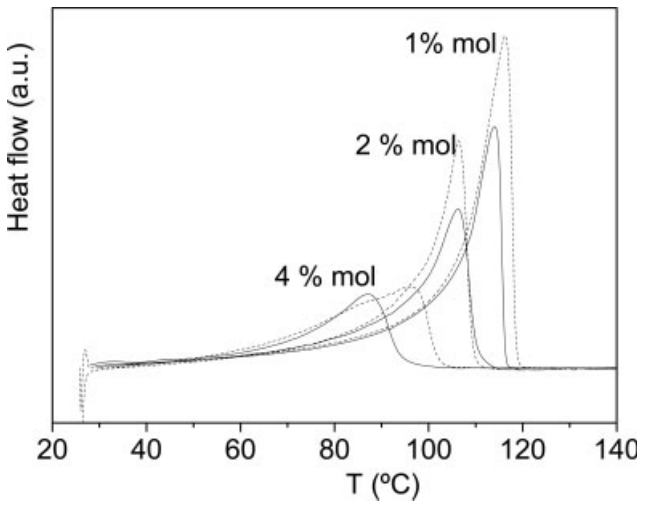

Figure 5 DSC melting thermograms of poly(ethylene-*co*-styrene) with different styrene contents produced by different catalysts: solid lines corresponds to polymers obtained from the NIT catalyst and dashed lines corresponds to polymers produced by the CGC catalyst.

The changes observed in melting peak temperatures obtained from the first heating thermograms versus the molar comonomer content are shown in Figure 6(a). As expected, a systematic decrease is shown in the melting temperature dependence on comonomer content in the copolymers generated using this new SSC catalyst system. The comparison with other ethylene-*co*-styrene copolymers obtained from SSC in our laboratory and from the literature, gives rise to very similar results.[11,15–17,27–29] Figure 6(b), showing the plot of crystallinity against molar comonomer content, reveals the characteristic exponential dependence in both families of copolymers, but also some important differences. The cristallinity follows the empirical equation $\alpha = \alpha_0 \exp(-bX_s)$, with X_s the molar comonomer fraction, where the constant b is 0.27 for NIT samples and 0.19 for CGC samples. This means that the melt enthalpy of the samples obtained from NIT catalyst decreases with respect to the CGC catalyst counterparts with the same styrene content. Even the homopolymers obtained from the NIT catalyst shows a characteristic low value of the crystallinity. The crystal content was measured in samples with the same thermal history, which means that nonequilibrium conditions are present. The crystallization time is the same for all samples, but due to the extremely large number of entanglement per molecule in the NIT samples (M_w increases 3–4 times with respect to those obtained from the CGC catalyst), the quasi-equilibrium crystallization would take very long time, as chain movements are much more restrained. For the samples obtained with the CGC catalyst, the crystallization time is probably sufficient to reach a quasi-equilibrium state, in spite of these samples also contain a fraction of long chain branches (i.e. a fraction of molecules with very long relaxation times), as it has been recently demonstrated by us in a separate work.[17,18]

The ethylene-*co*-styrene samples used in the studies of the group of Baer and coworkers,[27–29] are also plotted in Figure 6(b). These materials have substantially ''pseudo random'' incorporation of styrene as shown by ^{13}C nuclear magnetic resonance (^{13}C-NMR) analysis in their studies, and as occurs in the samples obtained by us using the CGC catalyst. Moreover, the samples studied by these authors also contained a certain amount of styrene homopolymer (PS) (up to 10

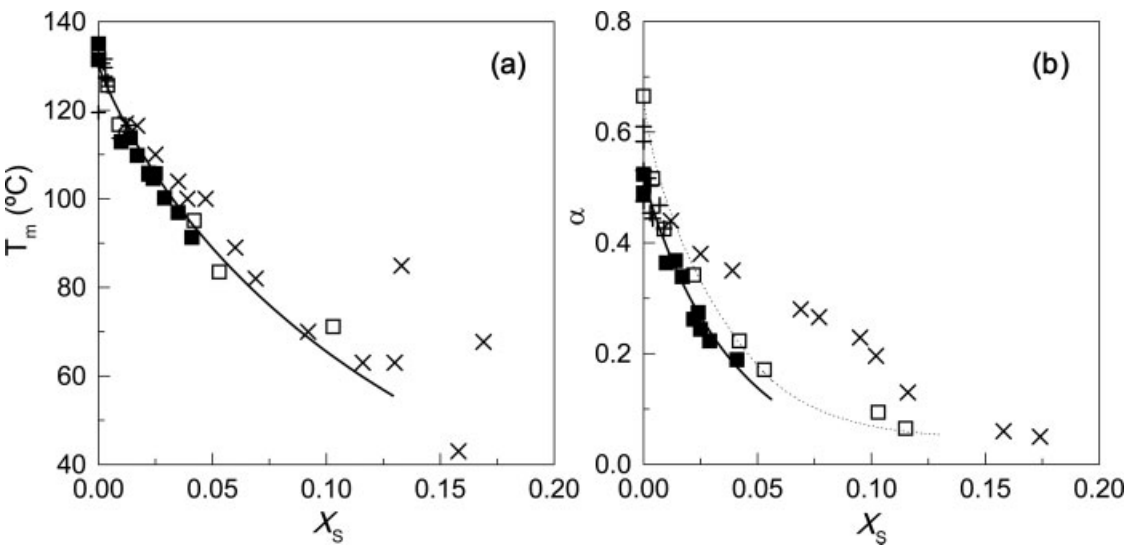

Figure 6 (a) Melting temperature versus molar comonomer fraction in ethylene-*co*-styrene samples: (■) NIT copolymers; (□) CGC copolymers; (+[15–17], ×[13,27–29]) SSC copolymers from the literature; (b) Crystallinity versus molar comonomer fraction in ethylene-*co*-styrene samples. The symbols are the same as in (a).

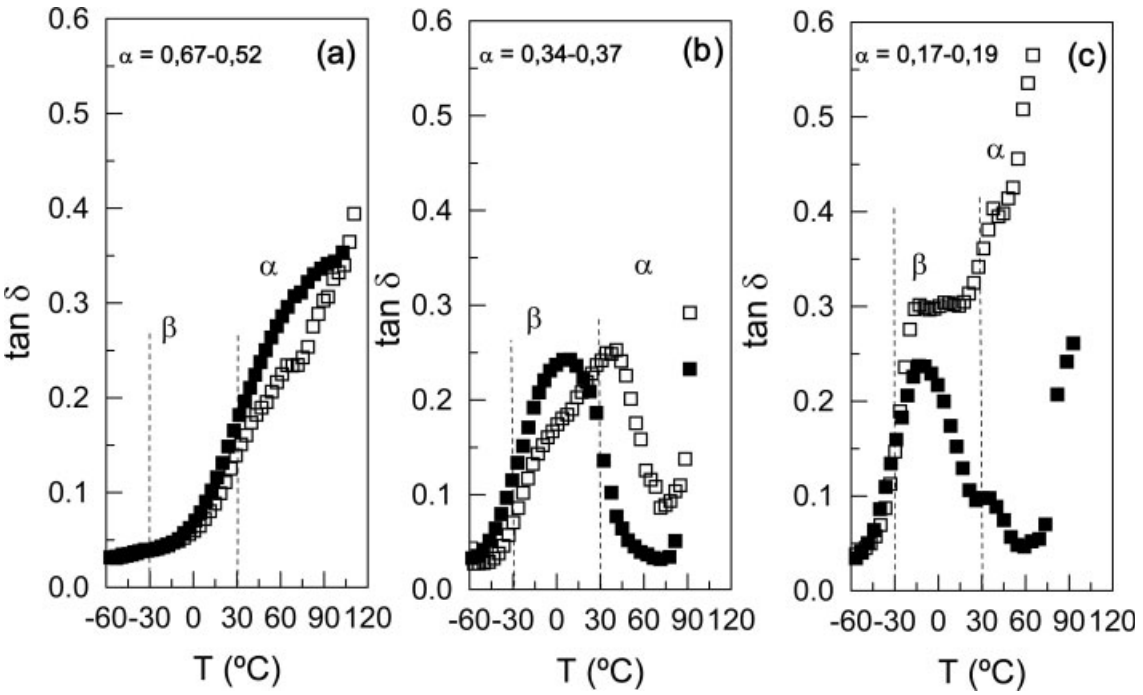

Figure 7 Loss tangent, tan δ, versus temperature curves for selected materials at fixed crystal content values. (a) Homopolymers with $\alpha > 0.50$; (b) Copolymers wit $\alpha \sim 0.35$; (c) Copolymers with $\alpha \sim 0.20$.

wt %), and inorganic additives in some cases, which can substantially alter the microstructure of the systems. Anyway, the general trends observed in Figure 6(a,b) reflect the progressive and similar decrease in the concentration and length of crystallizable ethylene sequences in both types of copolymers. This behavior is the expected for polymeric systems where comonomer was excluded from the crystal.

Dynamic-mechanical thermal analysis: mechanical properties

The dynamic mechanical relaxation spectra of six representative copolymers are shown in the form of loss tangent in Figure 7(a–c). The materials have been compared in order to their similar crystallinity. Figure 7(a) shows the result obtained for the homopolymer cases. In these samples, the main feature is the α transition, associated to the relaxation movements of chain segments along crystalline axis. For lower values of crystallinity than $\alpha = 0.4$, clear differences between both types of copolymers emerge [Fig. 7(b,c)]. For copolymers obtained from NIT catalyst very sharp and narrow β transitions develop, although in both types of copolymers the β temperature peak position remains constant around a value of $T_\beta = -10^\circ$C in the styrene content range explored. This result is clearly different from that obtained in ethylene/α-olefins, for which strong variations of T_β with comonomer content have been obtained. In general, in this kind of samples, β transition ranges between -25°C (for low comonomer content) and -70°C (for nearly amorphous samples).[30] A more complex response is seen in the copolymer obtained from CGC catalyst, pointing towards a more complicated microstructure. The strong variation of tan δ values at temperatures above the β transition could be related to the lower molecular weight of the samples. The wider relaxation in these samples suggests a wider distribution of chain rigidities or different coupling within the amorphous chains and the crystallites. The results obtained for these CGC samples are qualitatively in agreement to that reported in the literature for copolymers with similar crystallinity obtained from a similar catalyst system. The molecular weight of the samples from the literature is higher than those of our samples. This fact can explain the differences found in the linear viscoelastic fingerprint.[28]

The tensile stress–strain curves of some of the copolymers obtained from the two catalyst systems can be observed in Figure 8. In general, the homopolymers and copolymers studied content exhibited a yield maximum in the tensile stress–strain curve that coincided with the start of a well-defined neck during tensile testing at all the testing rates. The materials with the highest crystallinity behave as typical semicrystalline thermoplastics with the characteristic yielding and cold drawing phenomena. However, the sample with the highest molecular weight (homopolymer sample obtained from NIT catalyst) develops a characteristic strain hardening behavior at high strain

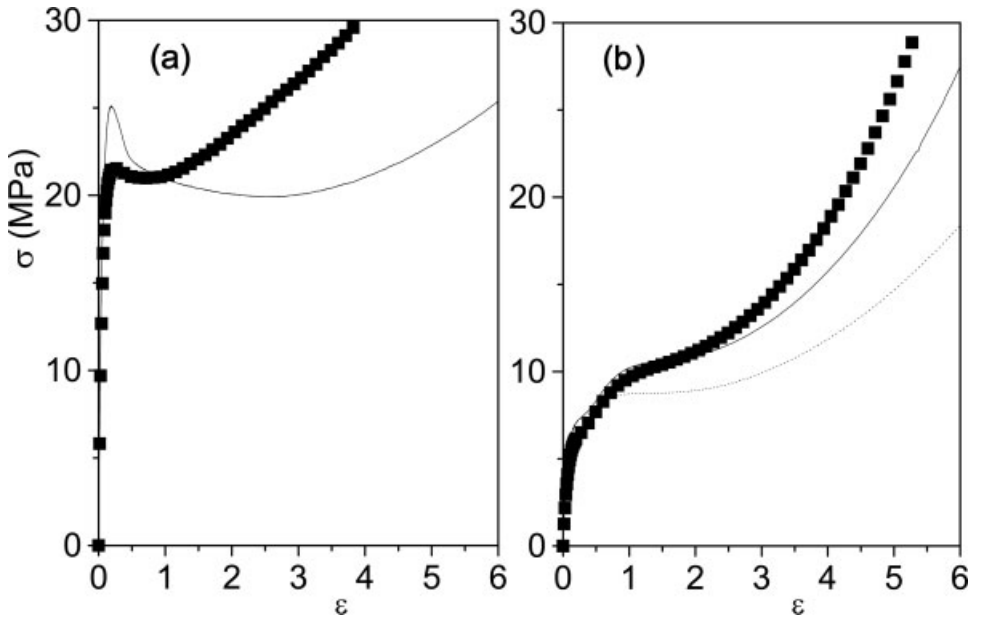

Figure 8 True tension stress–strain curves for selected copolymers with comparable crystal content. (a) Solid line corresponds to CGC homopolymer and symbols to NIT homopolymer. (b) Copolymers with a crystal content of $\alpha \sim 0.3$: solid line corresponds to CGC copolymer and symbols to NIT copolymer. The results obtained for an ethylene-*co*-1-hexene sample (dotted line) obtained from the CGC system is included for comparison.

values. The extremely large number of entanglements in the amorphous regions in these high molecular weight sample plays an important role, as they impose strong restriction to deformation in the high strain values region.[31] The copolymer obtained from NIT catalyst also shows a more pronounced strain hardening that the observed in its CGC counterpart. Moreover, the ethylene-*co*-styrene copolymers exhibit a much more pronounced sensitivity to stress response than ethylene-*co*-1-hexene copolymers obtained with the same catalyst in the same polymerization conditions. Chain extensibility (or flexibility) affects to the response of the material in this region, and then the local restrictions imposed by the bulky phenyl groups should play a role in the case of ethylene-*co*-styrene copolymers. The higher stress sensitivity of the ethylene-*co*-styrene copolymers in the high strain region becomes more pronounced as the crystallinity decreases, indicating that the amorphous component of the materials is increasingly involved in the deformation mechanism. Being segregated from the crystalline regions, the styrene has a strong effect on amorphous chain flexibility, and then chain extensibility, which becomes forced. These results are in agreement with those results obtained by Chang et al. when compared ethylene-*co*-styrene and ethylene-*co*-1-octene samples.[29]

Notwithstanding, the elastic modulus, obtained from the linear region at very small deformations and yield stress are the same at a given crystal content in both type of copolymers. As it is observed in Figure 8 the stress–strain curve in this region is independent not only on the type of catalyst system but also on the type comonomer. We have confirmed these results by measuring the flexural modulus in the dynamic mode within the linear viscoelastic region at a frequency of 1 Hz. In Figure 9 the first derivative of the flexural dynamic stress, $|\sigma_f^*|$ versus the dynamic flexural strain, ε_f, is plotted for some of the copolymers obtained by means of the NIT catalyst. Two interesting features can be obtained from these results: the elastic modulus in

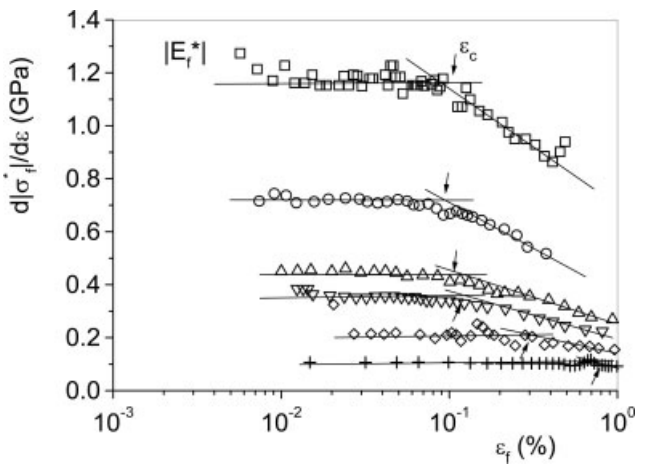

Figure 9 First derivative of the flexural dynamic stress to the flexural strain of some of the NIT samples studied. (□) NIT000, (○) NIT010, (△) NIT017, (▽) NIT025, (◇) NIT029, and (+) NIT041. The lines are drawn to give an estimation of the critical strain for the nonlinear behavior, ε_c, as indicated by the arrows.

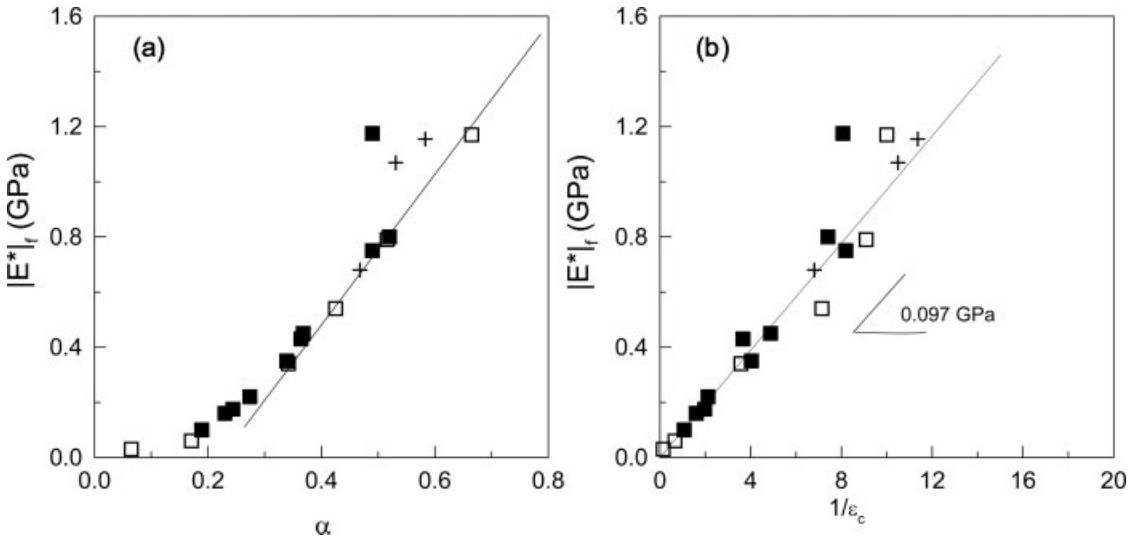

Figure 10 (a) Flexural modulus versus crystal content and (b) flexural modulus versus the reciprocal critical strain of all copolymer studied in this work. The symbols are the same as in Figures 4 and 6.

the linear viscoelastic region, $|E_f^*|$ and the critical strain, ε_c, for the onset of the non-linear behavior. A systematic decrease of the elastic modulus with crystallinity is observed in Figure 10(a), in a similar way to other results in the literature.[32–37] With the comonomer excluded from the crystals, the crystalline phase contains only long enough to crystallize methylene sequences, very active at small deformations even for elastomeric copolymers with the lowest crystallinity. It is more interesting to note that as the crystal content in the sample decreases the critical deformation for the onset of nonlinear behavior thoroughly increases. This trend is not arbitrary, as a relationship exists between the flexural modulus in the linear region and the reciprocal critical strain, as it is clearly seen in Figure 10(b). This last result is very remarkable, and it suggests that the deformation mechanisms and the linear viscoelastic limit are controlled by the applied stress. This limit is given by the slope of the straight line in Figure 10(b), which takes a value of around 0.097 $\pm$ 0.003 GPa.

Those materials with the highest M_w values seem to deviate from the correlations. These materials present very high values of the modulus, much more than the expected given the relatively low value of crystallinity. The cause of these increased values must be in an especially complex microstructure.[38] As molecular weight increases the lamellae become shorter and randomly arranged. Moreover, the amorphous phase in these samples is extremely entangled and rigid, as it is shown by the strain-hardening phenomenon observed in tensile stress–strain measurements. This rigidity of the amorphous zones between highly segmented crystallites probably could enhance the deformation resistance at low strains, giving rise to these characteristic higher values of the elastic modulus.

CONCLUSIONS

A set of ethylene-*co*-styrene samples obtained from a new single-site metallocene catalyst system has shown an extremely homogeneous molecular structure. The random and homogeneous molecular architecture remains in the samples as the amount of comonomer increases. This behavior clearly contrasts with the results obtained in other copolymers obtained by means of commercial constrained geometry catalyst, for which a clear broadening of the comonomer distribution is observed as the amount of comonomer increases in the copolymers. Very high molecular weight, characteristic of an ultra high molecular weight polyethylene in the homopolymer case, and narrow molecular weight distributions are also features of the materials obtained using this new catalyst system.

The molecular homogeneity leads to a characteristic homogeneous microstructure, as it is proved by the sharp and monomodal thermograms and mechanical transitions exhibited by these samples. The variation of the melting temperature and crystallinity with the styrene content suggest the exclusion of the bulky units from the crystal structure as occurs in other olefin-based copolymers. Tensile stress–strain curves show a characteristic strain hardening behavior as a product of the combination of the very high molecular weight of the samples and the bulky nature of the styrene units. These two factors, the extremely high concentration of entanglements in the amorphous phase and the enhanced local friction promoted by the phenyl groups, give rise to the

enhanced deformation resistance at high tensile strain values.

Nice correlations are found between the micro structural parameters and mechanical properties in the linear limit. As expected the elastic modulus depends on the crystal content, being modulated by the amorphous phase for those samples with the highest styrene content. An interesting result emerges when the characteristic features of the nonlinear regime are studied. It seems that this limit is mainly dependent on the stress generated in the sample during the deformation process, independently on the crystal content.

M.T. Expósito thanks the MEC for a Ph.D. fellowship (2003). J.F. Vega acknowledges the MEC for a Ramón y Cajal Tenure (2006).

References

1. Scheirs, J.; Kaminsky, W., Eds. Metallocene-Based Polyolefins, Vol. 1, Vol. 2; Wiley: New York, 1999.
2. Togni, A.; Halterman, R. L., Eds. Metallocenes: Synthesis, Reactivity and Applications, Vol. 1, Vol. 2; Wiley-VCH: New York, 1998.
3. Longo, P.; Grassi, A.; Oliva, L. Makromol Chem. 1990, 191, 2387.
4. Shapiro, P. J.; Bunel, E.; Schaefer, W. P.; Bercaw, J. E. Organometallics 1990, 9, 867.
5. Okuda, J. Chem Ber 1990, 123, 1649.
6. Stevens, J. C.; Timmers, F. J.; Wilson, D. R.; Schmidt, G. F.; Nickias, P. N.; Rosen, R. K.; Knight, G. W.; Lai, S. U.S. Pat EP0416815 (1991).
7. Carpenetti, D. W.; Kloppenburg, L.; Kupec, J. T.; Petersen, J. L. Organometallics 1996, 15, 1572.
8. Sernetz, F. G.; Mülhaupt, R.; Amor, F.; Eberle, T.; Okuda, J. J Polym Sci Part A: Polym Chem 1997, 35, 1571.
9. Sernetz, F. G.; Mülhaupt, R.; Waymouth, R. M. Macromol Chem Phys 1996, 197, 1071.
10. Thomann, Y.; Sernetz, F. G.; Thomann, R.; Kressler, J.; Mülhaupt, R. Macromol Chem Phys 1997, 198, 739.
11. Ren. J.; Hatfield, G. R. Macromolecules 1995, 28, 2588.
12. Oliva, L.; Caporaso, L.; Pellechia, C.; Zambelli, A. Macromolecules 1995, 28, 4665.
13. Arai, T.; Ohtsu, T.; Suzuki, S. Macromol Rapid Commun 1998, 19, 327.
14. Venditto, V.; De Tullio, G.; Izzo, L.; Oliva, L. Macromolecules 1998, 31, 4027.
15. Lobón-Poo, M.; Osío Barcina, J.; García Martínez, A.; Expósito, M. T.; Vega, J. F.; Martínez-Salazar, J.; Reyes, M. L. Macromolecules 2006, 39, 7479.
16. Haider, N.; Expósito, M. T.; Muñoz-Escalona, A.; Ramos, J.; Vega, J. F.; Méndez, L.; Martínez-Salazar, J. J Appl Polym Sci 2006, 102, 3420.
17. Expósito, M. T. PhD Thesis, Universidad Complutense de Madrid (Spain), 2006
18. Vega, J. F.; Expósito M. T; Martínez-Salazar, J.; Lobón-Poo, M.; Osío Barcina, J.; García Martínez, A.; Reyes, M. L. Macromolecules, submitted.
19. Quinn, F. A., Jr.; Mandelkern, L. J Am Chem Soc 1958, 80, 3178.
20. Martínez, S.; Expósito, M. T.; Ramos, J.; Cruz, V.; Martínez, M. C.; López, M.; Muñoz-Escalona, A.; Martínez-Salazar, J. J Polym Sci Part A: Polym Chem 2005, 43, 711.
21. Monrabal, B.; Blanco, J.; Nieto, J.; Soares, J. B. P. J Polym Sci Part A: Polym Chem 1999, 37, 89.
22. Sarzotti, D. M.; Soares, J. B. P.; Penlidis, A. J Polym Sci Part B: Polym Phys 2002, 40, 2595.
23. Anantawaraskul, S.; Soares, J. B. P.; Wood-Adams, P. A. J Polym Sci Part B: Polym Phys 2003, 41, 1762.
24. Bruaseth, I.; Soares, J. B. P.; Rytter, E. Polymer 2004, 45, 7853.
25. Anantawaraskul, S.; Soares, J. B. P.; Wood-Adams, P. A. Macromol Symp 2004, 206, 57.
26. Sarzotti, D. M.; Soares J. B. P.; Simon, L. C.; Britto, L. J. D. Polymer 2004, 45, 4787.
27. Chen, H.; Guest, M. J.; Chum, S.; Hiltner, A.; Baer, E. J Appl Polym Sci 1998, 70, 109.
28. Chen, H. Y.; Chum, S. P.; Hiltner, A.; Baer, E. J Polym Sci Part B: Polym Phys 2001, 39, 1578.
29. Chang, A.; Cheung, Y. W.; Hiltner, A.; Baer, E. J Polym Sci Part B: Polym Phys 2002, 40, 142.
30. Keating, M. I.; Lee, I.-H. J Macromol Sci Phys 1999, B38, 379.
31. Kennedy, M. A.; Peacock, A. J.; Mandelkern, L. Macromolecules 1994, 27, 5297.
32. Salazar, J. M.; Calleja, F. J. B. J Mater Sci 1983, 18, 1077.
33. Krigas, T. M.; Carella, J. M.; Struglinski, M. J.; Crist, B.; Graessley, W.W.; Schilling, F. C. J Polym Sci Polym Phys Ed 1985, 23, 509.
34. Popli, R.; Mandelkern, L. J Polym Sci Part B: Polym Phys 1987, 25, 441.
35. Crist, B.; Fisher, C. J.; Howard, P. R. Macromolecules 1989, 322, 1709.
36. Peacock, A. J.; Mandelkern, L. J Polym Sci Part B: Polym Phys 1990, 28, 1917.
37. Kennedy, M. A.; Peacock, A. J.; Mandelkern, L. Macromolecules 1994, 27, 5297.
38. Alom, Y.; Maram, G. Macromol Rapid Comm 2004, 25, 1378.